Journal of Advanced Ceramics
2016, **5**(4): 308–320
DOI: 10.1007/s40145-016-0204-2

ISSN 2226-4108
CN 10-1154/TQ

Research Article

Effect of nano- and micron-sized $K_{0.5}Na_{0.5}NbO_3$ fillers on the dielectric and piezoelectric properties of PVDF composites

Bharathi PONRAJ, Rajasekhar BHIMIREDDI, K. B. R. VARMA*

Materials Research Centre, *Indian Institute of Science*, *Bangalore-560012*, *India*

Received: June 09, 2016; Revised: July 25, 2016; Accepted: August 25, 2016

Abstract: Polymer nanocrystal composites were fabricated by embedding polyvinylidene fluoride (PVDF) with $K_{0.5}Na_{0.5}NbO_3$ (KNN) nanocrystallites of different volume fraction using the hot-pressing technique. For comparison, PVDF–KNN microcrystal composites of the same compositions were also fabricated which facilitated the studies of the crystallite size (wide range) effect on the dielectric and piezoelectric properties. The structural, morphological, dielectric, and piezoelectric properties of these nano and micro crystal composites were investigated. The incorporation of KNN fillers in PVDF at both nanometer and micron scales above 10 vol% resulted in the formation of polar β-form of PVDF. The room temperature dielectric constant as high as 3273 at 100 Hz was obtained for the PVDF comprising 40 vol% KNN nanocrystallites due to dipole–dipole interactions (as the presence of β-PVDF is prominent), whereas it was only 236 for the PVDF containing the same amount (40 vol%) of micron-sized crystallites of KNN at the same frequency. Various theoretical models were employed to predict the dielectric constants of the PVDF–KNN nano and micro crystal composites. The PVDF comprising 70 vol% micron-sized crystallites of KNN exhibited a d_{33} value of 35 pC/N, while the nanocrystal composites of PVDF–KNN did not exhibit any piezoelectric response perhaps due to the unrelieved internal stress within each grain, besides the fact that they have less domain walls.

Keywords: polyvinylidene fluoride (PVDF); $K_{0.5}Na_{0.5}NbO_3$ (KNN); composites; β-PVDF; nanocrystallites

1 Introduction

Polymer-based composites are of technological importance especially for energy storage applications [1–4]. The most commonly used host polymer is polyvinylidene fluoride (PVDF), which is being studied in great detail [5–10] owing to its multifarious applications. It is a semi-crystalline polymer existing in five polymorphic forms, namely α, β, γ, δ, and ε [9–11]. Amongst these, β-phase is polar, consisting of a planar zigzag all trans (TTTT) chain conformation with an orthorhombic structure (a = 8.58 Å, b = 4.91 Å, and c = 2.56 Å, space group $Cm2m$) [12,13]. It possesses spontaneous polarization and, as a result, exhibits piezoelectric and ferroelectric properties associated with high dielectric breakdown strength [14]. However, these properties are quite inferior to those of well known ferroelectric ceramics namely PZT, $BaTiO_3$,

* Corresponding author.
E-mail: kbrvarma@mrc.iisc.ernet.in

$PbTiO_3$, etc. [8]. These polymers are easy to process and more flexible, which makes them useful for fabricating flexible miniaturized devices [15]. However, the chief impediment in exploring PVDF for certain device applications is its inferior physical properties that include the dielectric, ferroelectric, and piezoelectric. Therefore, it is of industrial need and importance to improve these properties. One of the ways to improve the dielectric and piezoelectric characteristics of the polymer without losing its mechanical strength would be to fabricate PVDF-based composites comprising materials with superior physical properties.

Indeed, PVDF composites comprising $PbTiO_3$ and PZT were fabricated which exhibited high dielectric constant, large remnant polarization, improved piezoelectric properties, and high dielectric breakdown strength [16–18]. These composites find applications in electromechanical transducers such as underwater acoustic transducers, medical diagnostic transducers, tactile sensors, vibration testing, damage detection sensors, etc. [5–10,19]. However, lead-free and environmentally friendly materials are indispensable for aforementioned applications. Therefore, researchers around the globe have been directing their research efforts towards lead-free materials that exhibit physical properties akin to those of PZT-based ceramics [20–25]. Keeping this in view, we have used lead-free $K_{0.5}Na_{0.5}NbO_3$ (KNN) crystallites as fillers or dispersoids at different length scales in PVDF in order to obtain polymer nano and micro crystal composites. We believe that KNN ceramics have the potential to be considered in place of lead-based piezoelectric materials because of their good electromechanical properties ($k_p = 0.36$, $d_{33} = 80$ pC/N) associated with a high Curie temperature (T_C) [26]. They exhibit a morphotropic phase boundary (MPB) at 50% K and 50% Na, leading to a large piezoelectric response and high dielectric constant [27–31]. Also, recent reports on PVDF combined with 0.948KNN–0.052LS (KNNLS), $0.942(K_{0.480}Na_{0.535})NbO_3$–$0.058LiNbO_3$ (KNNLN), and $K_{0.48}Na_{0.52}NbO_3$-based composites (70:30) are interesting from their piezoelectric response view point. These were reported to have exhibited piezoelectric coefficients respectively as high as 25, 35, and 15 pC/N under normal poling conditions [32]. Similar reports on PVDF with 80 vol% of $(K_{0.44}Na_{0.52}Li_{0.04})(Nb_{0.86}Ta_{0.10}Sb_{0.04})O_3$ showed a maximum piezoelectric response of 35 pC/N [33]. However, no reports exist in the literature on the piezoelectric and related properties of PVDF composites comprising MPB-based pure $K_{0.5}Na_{0.5}NbO_3$ (KNN) crystallites at any length scales. Therefore, we thought that it was worth attempting to study the piezoelectric response of PVDF–KNN-based composites.

It is well known that the method of preparation of composites has a strong influence on their physical properties [18]. Several methods such as hot-pressing, compression molding, solvent casting, and tape casting (to fabricate in the form of thin sheets) besides the process associated with pellet shaped specimens were reported in the literature to fabricate several forms of polymer-based composites [17,18,34–40]. Among them 0–3 composites are found to be easy to process and could be produced in large scale which consist of polymers and randomly distributed ceramic particles [5,37]. The method that was reported in the literature to fabricate PVDF comprising KNNLS, KNNLST, and $K_{0.48}Na_{0.52}NbO_3$ was based on cold-pressing which generally results in the formation of voids and pores within the composites that affect the physical properties [32,33]. However, there are no reports available in the literature to fabricate the above composites based on hot-pressing technique. The hot-pressing technique is expected to yield dense composites associated with uniform microstructures as compared to that of the other techniques [37,39]. Therefore, in the present work, we have adopted simple hot-pressing method to fabricate 0–3 type composites in the form of pellets by using crystalline KNN powder as fillers in the PVDF matrix. Interestingly, this method facilitated PVDF to crystallize in polar β-PVDF with the addition of KNN fillers at optimum pressure and temperature. Besides the phase transition behavior of PVDF, the effect of crystallite size and volume fraction on the dielectric and piezoelectric properties of PVDF–KNN composites were investigated. For this, nano and micro crystal composites were fabricated separately by dispersing KNN at nanometer and micron scales in the PVDF matrix. It is known in the literature that the volume fraction of filler plays a crucial role in obtaining high dielectric constant and large piezoelectric response [18,41–44]. Therefore, we have varied the volume fraction of nano and micro crystalline KNN powder (as the case may be) in PVDF matrix in order to optimize the volume fraction that is required to obtain improved physical properties. In the case of microcrystal composites, we have varied the volume fraction from 10 to 70 vol%, whereas in the case of nanocrystal composites the volume was limited to 40 vol% due to difficulties involved in obtaining the samples in pellet form.

2 Experimental

2. 1 Preparation of KNN nanocrystalline powder

Fine nanocrystallites of KNN were synthesized via the citrate-assisted sol–gel method [45]. For this, analytical grade ammonium niobate (V) oxalate penta hydrate ($NH_4[NbO(C_2O_4)_2]\cdot 5H_2O$, H.C. Starck GmbH), anhydrous citric acid ($C_6H_8O_7$, Sigma-Aldrich), hydrogen peroxide (H_2O_2, 30% *w*/*v*, SDFCL), ammonia solution (SDFCL), sodium acetate (CH_3COONa, Fisher Scientific Co.), and potassium acetate (CH_3COOK, 99.5%, Alfa Aesar) were used. To begin with, anhydrous citric acid (10 mmol) was added to a 15 mL aqueous solution of H_2O_2 (30%) and stirred until the citric acid was completely dissolved and yielded clear solution. Niobium ammonium oxalate (10 mmol) was added to the solution thus obtained and stirred for 2 h at 60 ℃. Then the 25% aqueous NH_4OH was added dropwise slowly to increase the pH up to about 8.5 and stirring continued for another 1 h in order to obtain a transparent viscous yellow niobate peroxo (V)–citrate solution. Sodium acetate (5 mmol) and potassium acetate (5 mmol) solutions were prepared separately using distilled water and these were added slowly to the above niobate peroxo (V)–citrate solution. The precursor solution was further heated at 60 ℃ and stirred for 4 h to get the water evaporated and obtain solid precursor powder. Nanocrystalline KNN powder was obtained by subjecting the precursor powder to calcination at 550 ℃ for 5 h.

2. 2 Preparation of micron-sized KNN powder

Polycrystalline powder consisting of micron-sized crystallites of $K_{0.5}Na_{0.5}NbO_3$ (KNN) was synthesized by the conventional solid-state reaction route. Analytical grade K_2CO_3, Na_2CO_3, and Nb_2O_5 were taken in a stoichiometric ratio and mixed with acetone and ball-milled for 5 h using zirconia balls to obtain a homogenous mixture. This mixture was dried and calcined at 900 ℃ for 5 h.

2. 3 Preparation of PVDF–KNN nano and micro crystal composites

The PVDF with KNN microcrystal composites of different volume fraction (10–70 vol%) and PVDF nanocrystal composites comprising KNN nanocrystalline powder of 10–40 vol% were prepared by the hot-pressing technique. For this, the appropriate amounts of either micron- or nano-sized crystallites of KNN were added to the PVDF powder and mixed thoroughly using a mortar and pestle in an acetone medium for 1 h. These mixtures were dried at room temperature before making pellet shaped specimens. The dried mixtures were taken in a die of 10 mm in diameter and hot-pressed at optimized conditions. Nearly 1 mm thick samples of PVDF and PVDF with KNN (micron- or nano-sized crystallites) of different volume fraction were obtained. The densities of these pellets were measured by the Archimedes method using xylene as the liquid medium.

2. 4 Characterization

The hot-pressed samples were subjected to X-ray powder diffraction (XRD, Pananalytical X-pert Pro) with Cu Kα radiation in the 2θ range of 20°–60°. A scanning electron microscope (SEM, FESEM, Inspect F50) was used to study the micro-structural aspects of the samples under investigation. In order to have an insight into the nature of dispersion of KNN in the PVDF matrix, cross-sectional SEM was carried out for fractured samples of PVDF–KNN nano and micro crystal composites. For making electrical measurements, the major surfaces of the pure KNN nanocrystalline ceramics and hot-pressed pellets were silver coated on both sides. The frequency dependent dielectric response was studied using an impedance analyzer (Agilent 4294A) by sweeping between 100 Hz and 100 MHz at room temperature. The piezoelectric coefficients of the samples were measured by the piezo-d_{33} meter (KCF tech). The dielectric breakdown voltage measurements were carried out on the pellets as per the procedure outlined in ASTM D149.

3 Results and discussion

3. 1 X-ray structural studies

Figure 1 shows the XRD patterns obtained for pure KNN (nanocrystalline powder), hot-pressed pure PVDF, and PVDF with KNN nanocrystallites of different volume fraction (10–40 vol%). The XRD pattern obtained for pure KNN is indexed to the orthorhombic cell using ICSD data. The XRD pattern (Fig. 1(b)) recorded for hot-pressed PVDF reveals sharp peaks at $2\theta = 17.7°$ (100), 18.3° (020), 19.9° (110), 33.1° (130), and 35.8° (200) corresponding to the α-phase of PVDF, and the broad peaks at $2\theta = 26.5°$ (022) and 38.6° (211)

are assigned to the γ-phase of PVDF [11,46–51]. In order to visualize the effect of the presence of nanocrystallites of KNN on the structural characteristics of PVDF, the XRD studies were carried out on PVDF comprising different volume fraction of KNN (Figs. 1(c)–1(f)). The PVDF embedded with KNN nanocrystalline powder below 20 vol% shows peaks corresponding to α-, γ-, and small traces of β-phases along with predominant peaks pertaining to KNN. Indeed, above 20 vol% of KNN nanocrystalline powder in the PVDF matrix shows interestingly a distinct diffraction peak at $2\theta = 20.7°$ (200) corresponding to β-phase [8,46,47,51] in addition to KNN peaks (Fig. 1(d)). This phase, being non-centrosymmetric, is expected to play a crucial role in facilitating these composites to exhibit piezoelectric and ferroelectric properties. The intensity of the peak corresponding to the β-phase (with respect to the α- and γ-phases of PVDF) is predominant and found to increase with increase in the volume fraction (10–40 vol%) of nanocrystallites of KNN in the PVDF matrix. Interestingly, the peaks corresponding to α- and γ-phases of PVDF are absent in the XRD patterns obtained for the samples containing above 20 vol% of KNN. This result demonstrates that the presence of nanocrystallites of KNN in PVDF promotes strong electrostatic interaction between KNN at nanoscale and the PVDF polymer especially at the interface, leading to the alignment of the PVDF matrix in the extended TTTT conformation and resulting in the β-phase. Similar behavior is observed in the PVDF with various fillers such as $BaTiO_3$, MWCNT, TiO_2, and ferrite-based composites [41,52–55]. It is known in the literature that high pressure favors β-phase formation of PVDF [10]. However, it is intriguing to note that the moderate pressure and temperature employed in the present study in the presence of nanocrystallites of KNN facilitate the formation of the β-phase of PVDF.

In order to investigate and confirm the crystallite size effect of KNN on the transformation of α-phase to β-phase and its physical properties, systematic experiments were conducted using micron-sized KNN. Figure 2 shows the XRD patterns obtained for micron-sized crystallites of KNN and hot-pressed samples with micron-sized KNN of different volume fraction in the PVDF matrix. The peak corresponding to the β-phase is observed for PVDF containing 20–50 vol% of KNN (micron-sized crystalline powder) along with KNN peaks (Figs. 2(c)–2(f)). For the PVDF comprising 50 vol% KNN and above, the intensity of the β-phase peak is reduced drastically (Figs. 2(g) and 2(h)). Furthermore, the XRD patterns recorded show

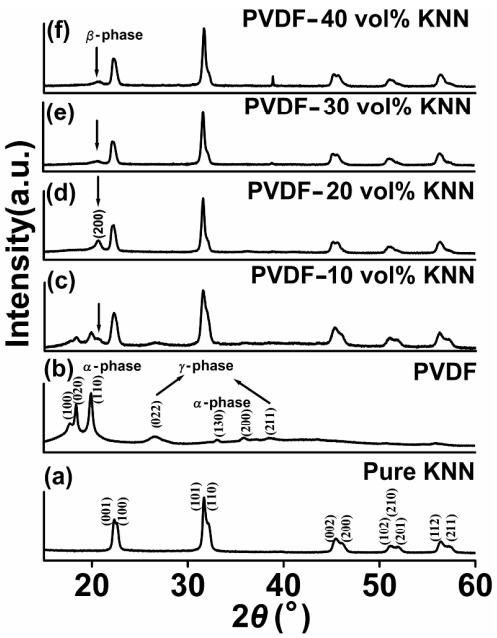

Fig. 1 XRD patterns for the hot-pressed PVDF–KNN nanocrystal composites: (a) KNN nanocrystalline powder, (b) hot-pressed PVDF, (c) PVDF–10 vol% KNN, (d) PVDF–20 vol% KNN, (e) PVDF–30 vol% KNN, and (f) PVDF–40 vol% KNN.

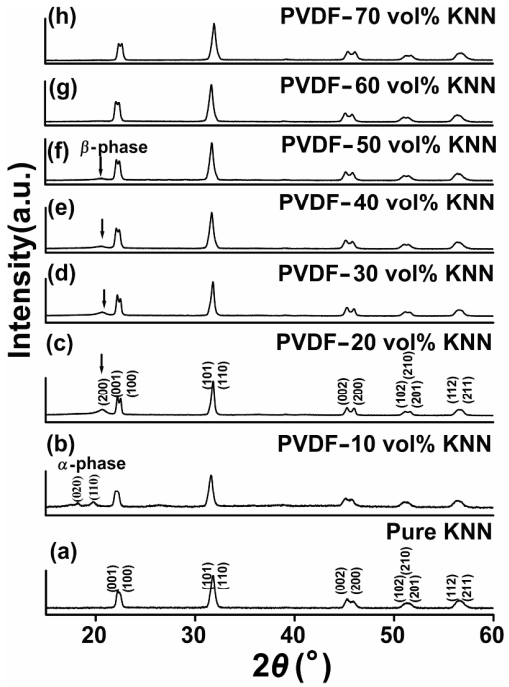

Fig. 2 XRD patterns for the hot-pressed PVDF–KNN microcrystal composites: (a) KNN powder containing micron-sized crystallites, (b) PVDF–10 vol% KNN, (c) PVDF–20 vol% KNN, (d) PVDF–30 vol% KNN, (e) PVDF–40 vol% KNN, (f) PVDF–50 vol% KNN, (g) PVDF–60 vol% KNN, and (h) PVDF–70 vol% KNN.

the presence of both PVDF and KNN phases, reflecting the composite nature of all the samples under study.

3. 2 Density and micro-structural studies

The densities of the PVDF–KNN nano and micro crystal composites were obtained both theoretically and experimentally, and these are depicted in Fig. 3. Theoretical values of PVDF–KNN nano and micro crystal composites were estimated using the mixture rule [18] given below:

$$\rho = V_f \rho_f + (1 - V_f)\rho_m \quad (1)$$

where ρ is the density of the composite, V_f is the volume fraction of filler (KNN nanopowder/micron-sized powder), ρ_f is the density of the filler (density of KNN, $\rho_f = 4.5$ g/cm^3), and ρ_m is the density of the matrix (density of PVDF matrix, $\rho_m = 1.78$ g/cm^3).

It is known in the literature that the composites prepared through the hot-pressing technique give the maximum possible density [17,37–40]. From the above equation, the composites with PVDF–KNN nanocrystals show the maximum relative density of 97% at lower volume fraction (10 vol%), whereas when the KNN nanocrystal content is increased from 10 to 20 vol%, the density decreases to 94% and remains almost constant above 20 vol%. This is attributed to the agglomeration of KNN nanocrystals at higher volume fraction (discussed in the later part). The microcrystal composites fabricated using the present method exhibit a maximum relative density of 96%–98% up to 50 vol%. For the KNN composition higher than 50 vol%, there is a sudden decrease in density. This is due to the poor dispersion of KNN microcrystals in the PVDF matrix at higher volume fraction of KNN micron-sized crystallites. The densities of the nano and micro crystal composites for all the composites under study were calculated by not taking the voids and defects into account. Figures 4 and 5 show the cross-sectional SEM micrographs recorded for nano and micro crystal composites, respectively. The SEM micrograph recorded for pure PVDF shows a smooth and continuous surface (Fig. 4(a)), and the SEM images of pure KNN nano and micro crystalline powder show the presence of well developed grains in 40–90 nm and 0.8–4 μm size ranges respectively, exhibiting a cuboidal morphology. The SEM micrographs along with the grain size distribution obtained for these samples are depicted in Fig. S1 in the Electronic Supplementary Material (ESM). There is a uniform distribution of KNN nanocrystallites in the PVDF matrix at lower volume fraction loading. The agglomeration of the crystallites increases with the increase in the volume fraction (beyond 10 vol%) of nanocrystallites of KNN in the PVDF matrix. Similarly, Fig. 5 shows the SEM micrographs obtained for the PVDF with different volume fraction of micron-sized KNN crystallites, depicting a homogenous distribution of micron-sized KNN crystallites in the PVDF matrix at lower volume fraction of KNN. The agglomeration of these crystallites is not that pronounced as compared to that of PVDF–KNN nanocrystal composites at higher loadings of KNN (Figs. 5(b)–5(g)). The connectivity of the crystallites is found to increase with an increase in the volume fraction of KNN in the PVDF matrix.

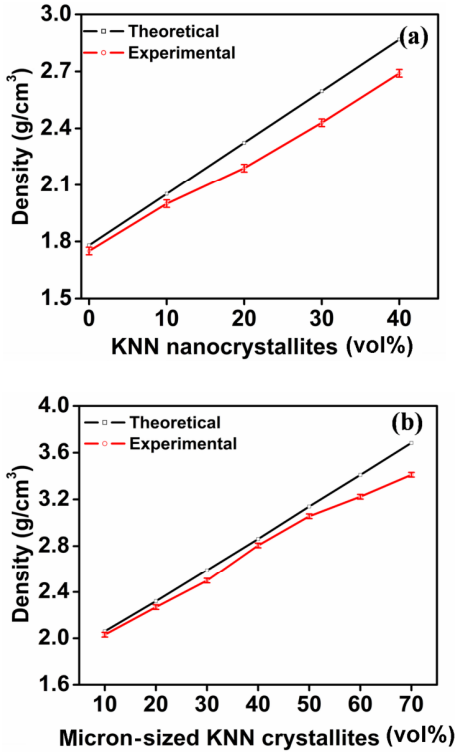

Fig. 3 Graphical representation of the variation of the density as a function of volume fraction for (a) nano- and (b) micron-sized KNN crystallites added to PVDF.

3. 3 Dielectric properties

Figure 6 shows the room temperature frequency dependent dielectric constant (ε_r) and loss (D) for PVDF with KNN nanocrystallites of different volume fraction in the frequency range of 100 Hz–100 MHz (covered in the present study). There is a decrease in the dielectric constant with an increase in frequency of measurement. The dielectric constant for pure PVDF is

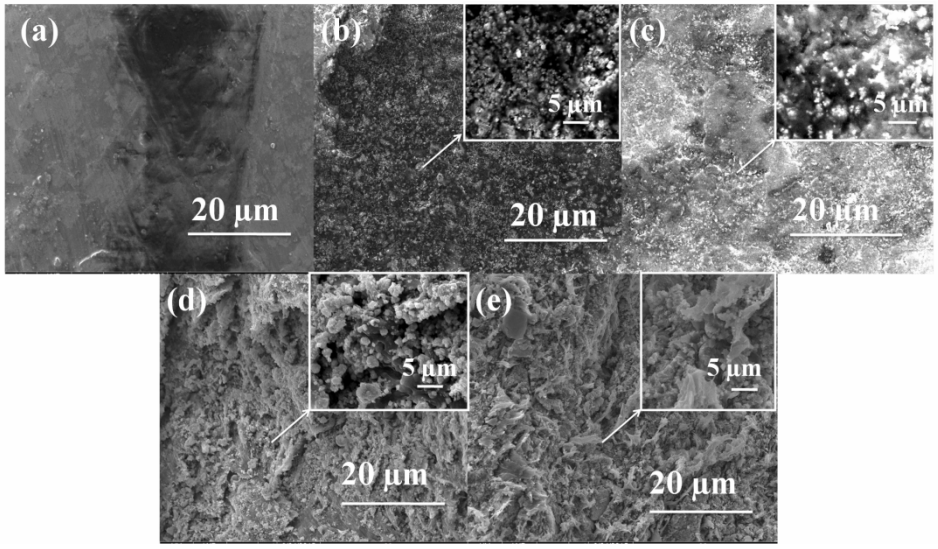

Fig. 4 Fractured cross-sectional SEM micrographs for hot-pressed PVDF–KNN nanocrystal composites: (a) hot-pressed PVDF, (b) PVDF–10 vol% KNN, (c) PVDF–20 vol% KNN, (d) PVDF–30 vol% KNN, (e) PVDF–40 vol% KNN, and the insets show the enlarged view of the corresponding images.

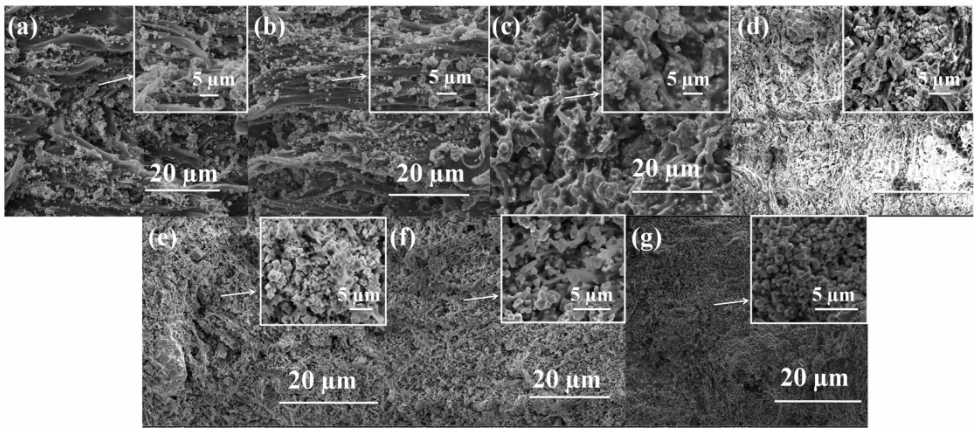

Fig. 5 Fractured cross-sectional SEM micrographs for hot-pressed PVDF–KNN microcrystal composites: (a) PVDF–10 vol% KNN, (b) PVDF–20 vol% KNN, (c) PVDF–30 vol% KNN, (d) PVDF–40 vol% KNN, (e) PVDF–50 vol% KNN, (f) PVDF–60 vol% KNN, (g) PVDF–70 vol% KNN, and the insets show the enlarged view of the corresponding images.

quite low as compared to that of KNN added PVDF samples. The value of dielectric constant for pure PVDF at 100 Hz is around 13.89. ε_r increases with the increase in volume fraction of KNN nanocrystallites in PVDF. ε_r is around 35.8 for 10 vol% KNN nanocrystallites and increased to a maximum value of 3273 for PVDF with 40 vol% KNN nanocrystals. The increase in ε_r with the increase in volume fraction is attributed to high density and the presence of maximum amount of β-PVDF (which is polar) coupled with high dielectric constant KNN nanocrystallites. Similarly, the dielectric loss versus frequency is obtained and low frequency dispersion is found to increase with an increase in the volume fraction of KNN nanocrystallites (up to 30 vol%) in the PVDF matrix, above which there is a sudden drop in the loss value. The loss (D) versus frequency shows two relaxations: one at low frequency region and the other at higher frequency (Fig. 6(b)). The relaxation at low frequency below 100 Hz is related to α_c relaxation associated with molecular motion in the crystalline regions of PVDF, whereas above 10^6 Hz, a small relaxation peak is observed due to glass transition relaxation of the PVDF and is referred to as α_a relaxation [46,47].

In order to study the effect of micron-sized crystallites of KNN on dielectric properties of PVDF, dielectric measurements were made at different frequencies for pure PVDF and PVDF with

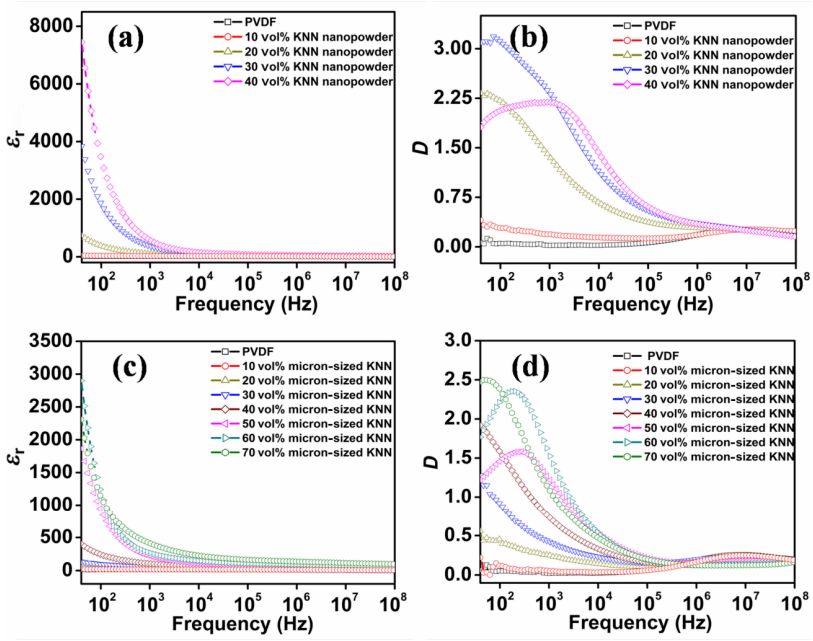

Fig. 6 Frequency dependent dielectric constant (ε_r) and loss (D) for (a, b) PVDF with KNN nano-sized crystallites of different volume fraction and (c, d) PVDF with KNN micron-sized crystallites of different volume fraction at room temperature.

micron-sized crystallites of KNN of different volume fraction (Fig. 6(c)). The dielectric constant decreases with an increase in frequency and, as expected, increases with an increase in the amount of KNN in the PVDF matrix. However, the value of the dielectric constant is low as compared to that of the PVDF–KNN nanocrystal composites. The increase in dielectric constant in the nanocrystal composites is chiefly attributed to an increase in dipole–dipole interaction between the PVDF polymer and the KNN nanocrystals at the interface and also due to ion–dipole interaction between the surface of the nanocrystallites and the PVDF matrix [18,54–58].

It is well known that, as the size of KNN crystallites decreases, there is a tendency of the nanocrystal to form agglomerates which results in the formation of continuous random cluster [56]. Therefore, one would expect an increase in strong dipole–dipole interaction between the large aggregates of KNN nanocrystallites and PVDF polymer at the interface resulting in an enhanced dielectric constant [56]. For instance, the value of ε_r for 10 vol% of micron-sized crystallites of KNN in the PVDF matrix is around 19 at 100 Hz and increases to 236 for 40 vol% loading, which is significantly low as compared to that of PVDF nanocrystal composites at 40 vol% loading. On further increasing the volume fraction of KNN to 70 vol%, ε_r reaches a value as high as 1096. The increase in ε_r for 70 vol% of PVDF–KNN microcrystal composite is mainly attributed to the increase in the volume fraction of the KNN micron-sized crystallites in the PVDF matrix vis-à-vis connectivity and strong dipole–dipole interaction. This attribution is evidenced by SEM studies (Fig. 5(g)). The room temperature values of dielectric constant (ε_r) obtained at 10 kHz for PVDF–KNN microcrystal composites are summarized in Table 1. The value of loss (D) observed in the present case is around 1.5 at 100 Hz for 40 vol% loading (Fig. 6(d)), which is quite low as compared to that of their nanocrystal composite counterpart (at 40 vol%) due to less agglomeration of crystallites.

To rationalize the dielectric properties of current

Table 1 Physical properties of PVDF–KNN microcrystal composites

Volume fraction of KNN micron-sized powder (vol%)	Piezoelectric coefficient d_{33} (pC/N)	Dielectric constant ε_r at 10 kHz	Figure of merit (FOM) (pm^2/N)	Breakdown voltage (kV)	Dielectric strength (kV/mm)
40	10	65.01	0.17	8.57	13.69
50	16	110.56	0.26	8.00	8.87
60	32	146.82	0.79	8.00	6.70
70	35	225.77	0.61	4.70	4.91

composites, various models were employed to predict their effective dielectric constants. The effective dielectric constant of the composite depends on the dielectric constant of the polymer, filler, filler size, filler shape, its volume fraction and also depends mainly on the dielectric constant of the interphase region, and the volume of the interphase region of the composite [18,46,47]. Therefore, to predict the dielectric constant of the PVDF–KNN nano and micro crystal composites, various models were used and these are given below.

According to the Maxwell and Garnett model, the effective dielectric constant (ε_r) of a composite comprising randomly dispersed crystallites having spherical morphology associated with a relatively high dielectric constant [42,59] is given by

$$\varepsilon_r = \varepsilon_1 \left\{ 1 + \frac{3q[(\varepsilon_2 - \varepsilon_1)/(\varepsilon_2 + 2\varepsilon_1)]}{1 - q[(\varepsilon_2 - \varepsilon_1)/(\varepsilon_2 + 2\varepsilon_1)]} \right\} \quad (2)$$

where ε_1 is the dielectric constant of the polymer (dielectric constant of PVDF, $\varepsilon_1 = 13.26$ at 10 kHz), ε_2 is the dielectric constant of the filler (dielectric constant of KNN nanocrystals, $\varepsilon_2 = 385$ at 10 kHz (Fig. S2 in the ESM) and for micron-sized KNN crystallites, it is 199 [60]), and q is the volume fraction of the filler.

The second model was proposed by Furukawa, in which, it was assumed that the filler crystallites are spherical and uniformly dispersed in the polymer matrix. It was proposed that the dielectric constant of the composite mainly depends on the dielectric constant of the matrix [44,61]. The effective dielectric constant in this model is given by

$$\varepsilon_r = \frac{1 + 2q}{1 - q} \varepsilon_1 \quad (3)$$

where ε_1 is the dielectric constant of the polymer matrix and q is the volume fraction of the spherical crystallites.

The third model that was used to predict the dielectric constant is due to Rayleigh [42], developed using the Maxwell–Garnett and Furukawa models for composite containing minor spherical fillers. The effective dielectric constant (ε_r) is given by

$$\varepsilon_r = \frac{2\varepsilon_1 + \varepsilon_2 - 2q(\varepsilon_1 - \varepsilon_2)}{2\varepsilon_1 + \varepsilon_2 + q(\varepsilon_1 - \varepsilon_2)} \varepsilon_1 \quad (4)$$

In order to account for the local variations of the electric field and the interaction with the applied electric field, the Bhimasankaram–Suryanarayana–Prasad (BSP) model was used. This model is very effective especially for the composite with a large fraction of piezoelectric crystallites [62]. The effective dielectric constant (ε_r) is given by

$$\varepsilon_r = \frac{\varepsilon_1(1-q) + \varepsilon_2 q\left(\frac{3\varepsilon_1}{\varepsilon_1 - \varepsilon_2}\right)\left[1 + \frac{3q(\varepsilon_2 - \varepsilon_1)}{\varepsilon_2 + 2\varepsilon_1}\right]}{(1-q) + q\left(\frac{3\varepsilon_1}{\varepsilon_2 + 2\varepsilon_1}\right)\left[1 + \frac{3q(\varepsilon_2 - \varepsilon_1)}{\varepsilon_2 + 2\varepsilon_1}\right]} \quad (5)$$

Apart from other models, the logarithmic mixture rule, the effective medium theory (EMT), and the Yamada model were also used to predict the dielectric constant of the composites under study using Eqs. (6), (7), and (8), respectively [42]:

$$\log \varepsilon_r = \delta_1 \log \varepsilon_1 + \delta_2 \log \varepsilon_2 \quad (6)$$

$$\varepsilon_r = \varepsilon_1 \left\{ 1 + \frac{q(\varepsilon_2 - \varepsilon_1)}{\varepsilon_1 + n[(1-q)(\varepsilon_2 - \varepsilon_1)]} \right\} \quad (7)$$

where δ_1 and δ_2 are volume fractions of PVDF and KNN nano-/micron-sized fillers (as the case may be) respectively, ε_1 and ε_2 are the dielectric constants of PVDF and KNN nano-/micron-sized fillers respectively, and n is the fitting parameter or the morphology factor. The EMT model is similar to the Maxwell–Garnett theory proposed for filler particles which are homogenously distributed, non-interacting and roughly spherical, and are surrounded by a concentric matrix layer. However, the Yamada model [63] has an advantage as it helps in predicting the dielectric constant of the composite based on the dielectric constant of the individual materials and it also considers a factor $n = 4\pi/m$, where n is related to the shape parameter or fitting parameter attributed to the shape of the filler particles and m is the relative orientation of the filler [42]. The dielectric constant (ε_r) of the composite according to the Yamada model is as follows:

$$\varepsilon_r = \varepsilon_1 \left\{ 1 + \frac{nq(\varepsilon_2 - \varepsilon_1)}{n\varepsilon_1 + [(1-q)(\varepsilon_2 - \varepsilon_1)]} \right\} \quad (8)$$

Using the above models, the effective dielectric constants of PVDF–KNN nano and micro crystal composites for different volume fraction of KNN were estimated and are depicted in Fig. 7 along with the corresponding experimental values. Figure 7(a) clearly shows that the models described in Eqs. (2)–(5) are ineffective for the PVDF with KNN nano-sized crystallites as the experimental values are not in agreement with those predicted by these models. However, the experimental dielectric constant values of nanocrystal composites are very close to those predicted

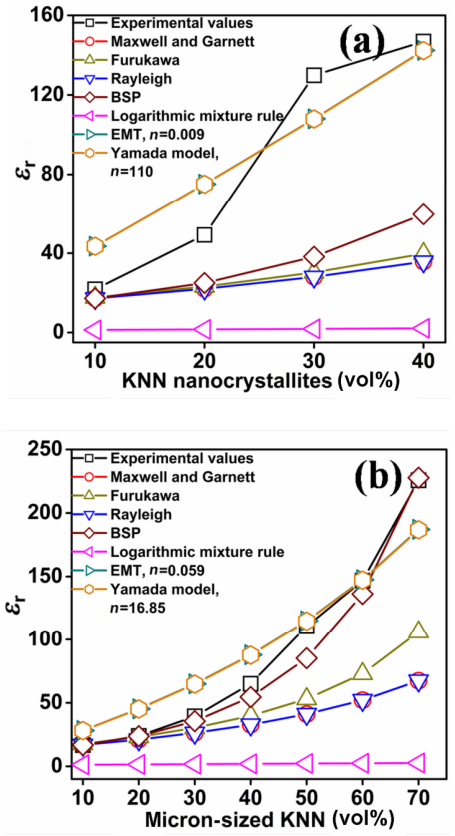

Fig. 7 Variation of the dielectric constant (ε_r) measured at room temperature and a frequency of 10 kHz: (a) PVDF–KNN nanocrystal composites and (b) PVDF–KNN microcrystal composites. For comparison, corresponding theoretical values obtained using various models are also shown.

by Yamada and EMT models, especially at higher concentrations of KNN nanocrystals. In the case of microcrystal composites, the values obtained by the models (2)–(5) are in good agreement for lower volume fraction (<40 vol%), whereas for higher volume fraction, the experimental values are in deviation. Indeed, the observed dielectric constants are in close agreement with those predicted by the Yamada model at higher volume fraction of KNN micron-sized crystallites in PVDF matrix (above 40 vol%) by taking into account the shape factor. The shape factor or fitting parameter is different for different particle size [18]. The shape factor reflects asymmetry, orientation, and distribution of the ceramic particles in the matrix. In the case of PVDF–KNN nanocrystal composites, n value is found to be high ($n=110$) as compared to that of PVDF–KNN microcrystal composites ($n=16.85$) as obtained from the best fit. This could be due to non-uniform distribution and/or clustering of KNN nanocrystallites in the PVDF matrix as compared to that of PVDF–KNN microcrystal composites [64].

3. 4 Piezoelectric and breakdown voltage studies

The crystallite size and volume fraction dependent piezoelectric properties were probed for PVDF–KNN nano and micro crystal composites. All the samples under study were poled at 3 kV/mm at room temperature and the piezoelectric coefficients were determined. It is well known in the literature that the piezoelectric coefficient has strong dependence on crystallite size [18,43,65]. Therefore, we have compared the results of the piezoelectric coefficient (d_{33}) obtained for hot-pressed PVDF with nano- and micron-sized crystallites of KNN at 40 vol% (exhibiting better piezoresponse). In the present study, the PVDF with 40 vol% of KNN nanocrystals does not show any piezoelectric response. However, the 40 vol% of KNN micron-sized crystallites dispersed in PVDF exhibits the interesting piezoelectric response (d_{33}) of 10 pC/N. The reason for PVDF–KNN nanocrystal composites (below 100 nm) not exhibiting piezoelectric properties is owing to the fact that these contain only a few domain walls, thus contribution from domain wall motion through poling is difficult due to internal clamping by space charge layer at the interface (between the matrix and the KNN nanocrystallites). Besides, the nanocrystallites have a tendency to agglomerate, which may give rise to an additional domain wall pinning effect at the grain boundaries of nanocrystals within the agglomerates [66]. Also, the size of the agglomerates increases with an increase in the volume fraction of nanocrystallites of KNN in the PVDF matrix. It may create a conduction path, where these space charges will percolate easily, resulting in high leakage current [67] and hindering the piezoelectric response of the nanocrystal composites.

In the case of the microcrystal composites, the agglomeration of crystallites is less pronounced and the surface area contact between the micron-sized KNN crystallites and the PVDF is large. Therefore, the poling of microcrystal composites would be more efficient than nanocrystal composites due to the increased probability of a large number of micron-sized crystallites getting poled and hence results in high d_{33} value [18]. In order to measure the piezoelectric response at different volume fraction, micron-sized KNN amounts are varied in different volume fraction (10–70 vol%) in PVDF matrix. The PVDF with micron-sized crystallites of KNN at lower volume

fraction (below 40 vol%) does not show significant piezoelectric response. When the volume fraction is increased to 40 vol% and above in PVDF, it exhibits enhanced piezoelectric response. The piezoelectric coefficient (d_{33}) is found to increase with an increase in the volume fraction of the micron-sized KNN crystallites in PVDF matrix. The PVDF microcrystal composite at 40 vol% shows a d_{33} value of 10 pC/N and reaches a maximum value of 35 pC/N for 70 vol% of KNN in the PVDF matrix (Fig. 8). The increase in the d_{33} coefficient with the increase in KNN content is attributed to an increase in the connectivity of crystallites, coupled with an enhanced degree of domain reorientation through poling [33].

In addition, in order to have a gross idea about the performance of piezo active PVDF–KNN microcrystal composites for energy harvesting applications, a figure of merit (FOM) is estimated using the following expression [33]:

$$\text{Figure of merit (FOM)} = \frac{d_{33}^2}{\varepsilon_0 \varepsilon_r} (\text{pm}^2/\text{N}) \qquad (9)$$

The figure of merit is found to increase with the increase in volume fraction of KNN up to 60 vol% in the PVDF matrix, and beyond this, there is a sudden drop in the value. This could be due to poor dispersion at higher volume fraction of KNN micron-sized fillers in the PVDF matrix and also due to a high dielectric constant (ε_r) value. Similar behavior was reported in the case of PVDF with 80 vol% of KNNLST composites [33].

The PVDF with different volume fraction of microcrystalline KNN (40–70 vol%) were subjected to breakdown tests according to ASTM D149 standard to estimate breakdown voltages and their dielectric strengths. These studies were carried out in air ambience. The sample was placed between two cylindrical electrodes (both top and bottom) of 6 mm in diameter and the AC (50 Hz) voltage was continuously increased at a rate of 500 V/s till the sample broke down [47]. The breakdown voltages V (kV) of the samples were recorded and the dielectric strengths E (kV/mm) were calculated as $E = V/t$, where t is the thickness of the sample in millimeter [47]. As expected, the breakdown voltage is found to decrease with an increase in volume fraction of KNN in the PVDF matrix. The breakdown voltage at 40 vol% of KNN in PVDF shows 8.56 kV and decreases to a value of 4.7 kV for 70 vol% of micron-sized crystallites. This is ascribed to charge leakage in the composites. It is known in the literature that addition of fillers to the polymer introduces defects in the sample which causes charge leakage and reduces the dielectric strength [67–69]. The dielectric strength, breakdown voltage, figure of merit, and their corresponding piezoelectric coefficient for PVDF–KNN microcrystal composites are summarized in Table 1.

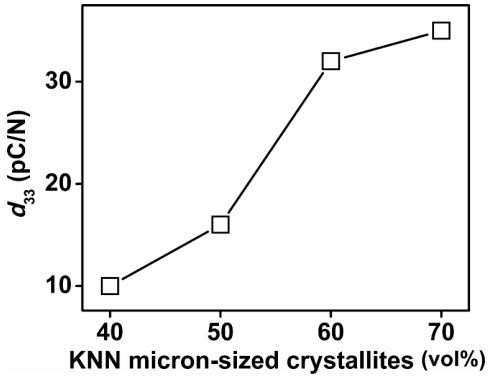

Fig. 8 Variation of the piezoelectric coefficient (d_{33}) as a function of the volume fraction of KNN crystallites at micron scale.

4 Conclusions

X-ray structural studies carried out on KNN added PVDF confirmed the transformation of PVDF to polar β-phase; this was particularly effective when KNN was at nanoscale. More than 10 fold enhancement in the dielectric properties was achieved in 40 vol% KNN nanocrystallites added PVDF ($\varepsilon_r = 3273$ at 100 Hz) as compared PVDF–KNN microcrystal composites. This was attributed to an increase in dipole–dipole interaction and ion–dipole interaction between the β-PVDF and KNN nanocrystals. The higher d_{33} value (35 pC/N) exhibited by 70 vol% KNN (micron-sized crystallites)–PVDF composite was of technological importance. This was rationalized by invoking the presence of a large number of domain variants, besides the increased connectivity of the KNN in the PVDF matrix. Though the PVDF–KNN nanocrystal composites did not exhibit piezoresponse, it would be of some interest for dielectric applications as it exhibited higher dielectric constants.

Acknowledgements

One of the authors, Rajasekhar Bhimireddi, acknowledges

the University Grants Commission, Government of India, for the financial support provided through Dr. D. S. Kothari's post-doctoral fellowship. Also, the authors are thankful to Dr. P. Thomas, Joint Director, CPRI, Bangalore, India, for helping in making dielectric breakdown voltage studies.

Electronic Supplementary Material: Supplementary material (SEM images for pure KNN nano- and micron-sized powder (Figs. S1(a) and S1(b)), and frequency dependent dielectric constant plot for pure KNN ceramics (Fig. S2)) is available in the online version of this article at http://dx.doi.org/10.1007/s40145-016-0204-2.

References

[1] Wang Q, Zhu L. Polymer nanocomposites for electrical energy storage. *J Polym Sci Pol Phys* 2011, **49**: 1421–1429.

[2] Siddabattuni S, Schuman TP. Polymer–ceramic nanocomposite dielectrics for advanced energy storage. In *Polymer Composites for Energy Harvesting, Conversion, and Storage*. Li L, Wong-Ng W, Sharp J, Eds. Washington, DC, USA: American Chemical Society, 2014: 165–190.

[3] Tan D, Irwin P. Polymer based nanodielectric composites. In *Advances in Ceramics—Electric and Magnetic Ceramics, Bioceramics, Ceramics and Environment*. Sikalidis C, Ed. InTech, 2011, DOI: 10.5772/23012.

[4] Barber P, Balasubramanian S, Anguchamy Y, *et al*. Polymer composite and nanocomposite dielectric materials for pulse power energy storage. *Materials* 2009, **2**: 1697–1733.

[5] Ramadan KS, Sameoto D, Evoy S. A review of piezoelectric polymers as functional materials for electromechanical transducers. *Smart Mater Struct* 2014, **23**: 033001.

[6] Chang J, Dommer M, Chang C, *et al*. Piezoelectric nanofibers for energy scavenging applications. *Nano Energy* 2012, **1**: 356–371.

[7] Varghese J, Whatmore RW, Holmes JD. Ferroelectric nanoparticles, wires and tubes: Synthesis, characterization and applications. *J Mater Chem C* 2013, **1**: 2618–2638.

[8] Bowen CR, Kim HA, Weaver PM, *et al*. Piezoelectric and ferroelectric materials and structures for energy harvesting applications. *Energy Environ Sci* 2014, **7**: 25–44.

[9] Li Z, Wang J, Wang X, *et al*. Ferro- and piezo-electric properties of a poly(vinyl fluoride) film with high ferro- to para-electric phase transition temperature. *RSC Adv* 2015, **5**: 80950–80955.

[10] Cui Z, Hassankiadeh NT, Zhuang Y, *et al*. Crystalline polymorphism in poly(vinylidenefluoride) membranes. *Prog Polym Sci* 2015, **51**: 94–126.

[11] Satapathy S, Pawar S, Gupta PK, *et al*. Effect of annealing on phase transition in poly(vinylidene fluoride) films prepared using polar solvent. *Bull Mater Sci* 2011, **34**: 727–733.

[12] Lando JB, Olf HG, Peterlin A. Nuclear magnetic resonance and X-ray determination of the structure of poly(vinylidene fluoride). *J Polym Sci Pol Chem* 1966, **4**: 941–951.

[13] Hasegawa R, Kobayashi M, Tadokoro H. Molecular conformation and packing of poly(vinylidene fluoride). Stability of three crystalline forms and the effect of high pressure. *Polym J* 1972, **3**: 591–599.

[14] Chen S, Yao K, Tay FEH, *et al*. Ferroelectric poly(vinylidene fluoride) thin films on Si substrate with the β phase promoted by hydrated magnesium. *J Appl Phys* 2007, **102**: 104108.

[15] Qi Y, McAlpine MC. Nanotechnology-enabled flexible and biocompatible energy harvesting. *Energy Environ Sci* 2010, **3**: 1275–1285.

[16] Kulek J, Hilczer B, Burianova L, *et al*. Dielectric, piezoelectric and pyroelectric response of $PbTiO_3$–PVDF composites. *J Korean Phys Soc* 1998, **32**: S1079–S1081.

[17] Seema A, Dayas KR, Varghese JM. PVDF–PZT–5H composites prepared by hot press and tape casting techniques. *J Appl Polym Sci* 2007, **106**: 146–151.

[18] Jain A, Prashanth KJ, Sharma AK, *et al*. Dielectric and piezoelectric properties of PVDF/PZT composites: A review. *Polym Eng Sci* 2015, **55**: 1589–1616.

[19] Chan HLW, Chen Y, Choy CL. A poling study of PZT/P(VDF-TrFE) copolymer 0–3 composites. *Integr Ferroelectr* 1995, **9**: 207–214.

[20] Luo B, Wang X, Zhao Q, *et al*. Synthesis, characterization and dielectric properties of surface functionalized ferroelectric ceramic/epoxy resin composites with high dielectric permittivity. *Compos Sci Technol* 2015, **112**: 1–7.

[21] Choy SH, Li WK, Li HK, *et al*. Study of BNKLBT-1.5 lead-free ceramic/epoxy 1–3 composites. *J Appl Phys* 2007, **102**: 114111.

[22] Sareein T, Thamjaree W, Nhuapeng W, *et al*. Fabrication of 0–3 non-lead based piezoceramic/polymer composites using suction technique. *Adv Mater Re*s 2008, **55–57**: 141–144.

[23] Jadidian B, Hagh NM, Winder AA, *et al*. 25 MHz ultrasonic transducers with lead-free piezoceramic, 1–3 PZT fiber-epoxy composite, and PVDF polymer active elements. *IEEE T Ultrason Ferr* 2009, **56**: 368–378.

[24] Le DT, Do NB, Kim DU, *et al*. Preparation and characterization of lead-free $(K_{0.47}Na_{0.51}Li_{0.02})(Nb_{0.8}Ta_{0.2})O_3$ piezoceramic/epoxy composites with 0–3 connectivity. *Ceram Int* 2012, **38**: S259–S262.

[25] Kumar P, Mishra P, Sonia S. Synthesis and characterization of lead-free ferroelectric $0.5[Ba(Zr_{0.2}Ti_{0.8})O_3]$–$0.5[(Ba_{0.7}Ca_{0.3})TiO_3]$–polyvinylidene difluoride 0–3 composites. *J Inorg Organomet Polym* 2013, **23**: 539–545.

[26] Egerton L, Dillon DM. Piezoelectric and dielectric properties of ceramics in the system potassium–sodium niobate. *J Am Ceram Soc* 1959, **42**: 438–442.

[27] Guo Y, Kakimoto K-i, Ohsato H. Phase transitional behavior and piezoelectric properties of $(Na_{0.5}K_{0.5})NbO_3$–$LiNbO_3$ ceramics. *Appl Phys Lett* 2004, **85**: 4121.

[28] Wu J, Xiao D, Wang Y, *et al*. Compositional dependence of phase structure and electrical properties in $(K_{0.42}Na_{0.58})NbO_3$–$LiSbO_3(K_{0.42}Na_{0.58})NbO_3$–$LiSbO_3$ lead-free ceramics. *J Appl Phys* 2007, **102**: 114113.

[29] Hollenstein E, Davis M, Damjanovic D, *et al*. Piezoelectric properties of Li- and Ta-modified $(K_{0.5}Na_{0.5})NbO_3$ ceramics. *Appl Phys Lett* 2005, **87**: 182905.

[30] Park H-Y, Ahn C-W, Song H-C, *et al*. Microstructure and piezoelectric properties of $0.95(Na_{0.5}K_{0.5})NbO_3$–$0.05BaTiO_3$ ceramics. *Appl Phys Lett* 2006, **89**: 062906.

[31] Wang K, Li J-F. (K,Na)NbO_3-based lead-free piezoceramics: Phase transition, sintering, and property enhancement. *J Adv Ceram* 2012, **1**: 24–37.

[32] Zhang P, Wang M, Zhu J, *et al*. Lead-free piezoelectric composites with high piezoelectric performance and high dielectric constant caused by percolation phenomenon. *J Mater Sci: Mater Electron* 2014, **25**: 4225–4229.

[33] Seol J-H, Lee JS, Ji H-N, *et al*. Piezoelectric and dielectric properties of $(K_{0.44}Na_{0.52}Li_{0.04})(Nb_{0.86}Ta_{0.10}Sb_{0.04})O_3$–PVDF composites. *Ceram Int* 2012, **38**: S263–S266.

[34] Janas VF, Safari A. Overview of fine-scale piezoelectric ceramic/polymer composite processing. *J Am Ceram Soc* 1995, **78**: 2945–2955.

[35] Shrout TR, Schulze WA, Biggers JV. Simplified fabrication of PZT/polymer composites. *Mater Res Bull* 1979, **14**: 1553–1559.

[36] Skinner DP, Newnham RE, Cross LE. Flexible composite transducers. *Mater Res Bull* 1978, **13**: 599–607.

[37] Venkatragavaraj E, Satish B, Vinod PR, *et al*. Piezoelectric properties of ferroelectric PZT–polymer composites. *J Phys D: Appl Phys* 2001, **34**: 487–492.

[38] Satish B, Sridevi K, Vijaya MS. Study of piezoelectric and dielectric properties of ferroelectric PZT–polymer composites prepared by hot-press technique. *J Phys D: Appl Phys* 2002, **35**: 2048–2050.

[39] Zhang D-Q, Wang D-W, Yuan J, *et al*. Structural and electrical properties of PZT/PVDF piezoelectric nanocomposites prepared by cold-press and hot-press routes. *Chinese Phys Lett* 2008, **25**: 4410–4413.

[40] Senthilkumar R, Sridevi K, Venkatesan J, *et al*. Investigations on ferroelectric PZT–PVDF composites of 0–3 connectivity. *Ferroelectrics* 2005, **325**: 121–130.

[41] Mendes SF, Costa CM, Caparros C, *et al*. Effect of filler size and concentration on the structure and properties of poly(vinylidenefluoride)/$BaTiO_3$ nanocomposites. *J Mater Sci* 2012, **47**: 1378–1388.

[42] Mendes SF, Costa CM, Sencadas V, *et al*. Effect of the ceramic grain size and concentration on the dynamical mechanical and dielectric behavior of poly(vinilidene fluoride)/$Pb(Zr_{0.53}Ti_{0.47})O_3$ composites. *Appl Phys A* 2009, **96**: 899–908.

[43] Lee H-G, Kim H-G. Ceramic particle size dependence of dielectric and piezoelectric properties of piezoelectric ceramic polymer composites. *J Appl Phys* 1990, **67**: 2024.

[44] Yamada T, Ueda T, Kitayama T. Piezoelectricity of a high-content lead zirconate titanate/polymer composite. *J Appl Phys* 1982, **53**: 4328.

[45] Stavber G, Malič B, Kosec M. A road to environmentally friendly materials chemistry: Low-temperature synthesis of nanosized $K_{0.5}Na_{0.5}NbO_3$ powders through peroxide intermediates in water. *Green Chem* 2011, **13**: 1303–1310.

[46] Thomas P, Varughese KT, Dwarakanath K, *et al*. Dielectric properties of poly(vinylidene fluoride)/$CaCu_3Ti_4O_{12}$ composites. *Compos Sci Technol* 2010, **70**: 539–545.

[47] Thomas P, Satapathy S, Dwarakanath K, *et al*. Dielectric properties of poly(vinylidene fluoride)/$CaCu_3Ti_4O_{12}$ nanocrystal composite thick films. *eXPRESS Polym Lett* 2010, **4**: 632–643.

[48] Malecki J, Hilczer B. Dielectric behaviour of polymers and composites. *Key Eng Mat* 1994, **92–93**: 181–216.

[49] Sekar R, Tripathi AK, Pillai PKC. X-ray diffraction and dielectric studies of a $BaTiO_3$:PVDF composite. *Mat Sci Eng B* 1989, **5**: 33–36.

[50] Muralidhar C, Pillai PKC. XRD studies on barium titanate ($BaTiO_3$)/polyvinylidene fluoride (PVDF) composites. *J Mater Sci* 1988, **23**: 410–414.

[51] Esterly DM, Love BJ. Phase transformation to β-poly(vinylidene fluoride) by milling. *J Polym Sci Pol Phys* 2004, **42**: 91–97.

[52] Kim GH, Hong SM, Seo Y. Piezoelectric properties of poly(vinylidene fluoride) and carbon nanotube blends: β-phase development. *Phys Chem Chem Phys* 2009, **11**: 10506–10512.

[53] An NL, Liu H, Ding Y, *et al*. Preparation and electroactive properties of a PVDF/nano-TiO_2 composite film. *Appl Surf Sci* 2011, **257**: 3831–3835.

[54] Martins P, Costa CM, Lanceros-Mendez S. Nucleation of electroactive *β*-phase poly(vinilidene fluoride) with $CoFe_2O_4$ and $NiFe_2O_4$ nanofillers: A new method for the preparation of multiferroic nanocomposites. *Appl Phys A* 2011, **103**: 233–237.

[55] Martins P, Costa CM, Benelmekki M, *et al*. On the origin of the electroactive poly(vinylidene fluoride) *β*-phase nucleation by ferrite nanoparticles via surface electrostatic interactions. *CrystEngComm* 2012, **14**: 2807–2811.

[56] Dang Z-M, Wang H-Y, Peng B, *et al*. Effect of $BaTiO_3$ size on dielectric property of $BaTiO_3$/PVDF composites. *J Electroceram* 2008, **21**: 381–384.

[57] Sarkar S, Garain S, Mandal D, *et al*. Electro-active phase formation in PVDF–$BiVO_4$ flexible nanocomposite films for high energy density storage application. *RSC Adv* 2014, **4**: 48220–48227.

[58] Kar E, Bose N, Das S, *et al*. Enhancement of electroactive *β* phase crystallization and dielectric constant of PVDF by incorporating GeO_2 and SiO_2 nanoparticles. *Phys Chem Chem Phys* 2015, **17**: 22784–22798.

[59] Luo B, Wang X, Wang Y, *et al*. Fabrication, characterization, properties and theoretical analysis of ceramic/PVDF composite flexible films with high dielectric constant and low dielectric loss. *J Mater Chem A* 2014, **2**: 510–519.

[60] Bharathi P, Varma KBR. Effect of the addition of B_2O_3 on the density, microstructure, dielectric, piezoelectric and ferroelectric properties of $K_{0.5}Na_{0.5}NbO_3$ ceramics. *J Electron Mater* 2014, **43**: 493–505.

[61] Furukawa T, Ishida K, Fukada E. Piezoelectric properties in the composite systems of polymers and PZT ceramics. *J Appl Phys* 1979, **50**: 4904.

[62] Bhimasankaram T, Suryanarayana SV, Prasad G. Piezoelectric polymer composite materials. *Current Sci*

1998, **74**: 967–976.
[63] Yamada T, Ueda T, Kitayama T. Piezoelectricity of a high-content lead zirconate titanate/polymer composite. *J Appl Phys* 1982, **53**: 4328–4332.
[64] Araújo MC, Costa CM, Lanceros-Méndez S. Evaluation of dielectric models for ceramic/polymer composites: Effect of filler size and concentration. *J Non-Cryst Solids* 2014, **387**: 6–15.
[65] Rujijanagul G, Boonyakul S, Tunkasiri T. Effect of the particle size of PZT on the microstructure and the piezoelectric properties of 0–3 PZT/polymer composites. *J Mater Sci Lett* 2001, **20**: 1943–1945.
[66] Paik H, Choi Y-Y, Hong S, *et al*. Effect of Ag nanoparticle concentration on the electrical and ferroelectric properties of Ag/P(VDF-TrFE) composite films. *Sci Rep* 2015, **5**: 13209.
[67] Dou X, Liu X, Zhang Y, *et al*. Improved dielectric strength of barium titanate–polyvinylidene fluoride nanocomposite. *Appl Phys Lett* 2009, **95**: 132904.
[68] Aulagner E, Guillet J, Seytre S, *et al*. (PVDF/$BaTiO_3$) and (PP/$BaTiO_3$) films for energy storage capacitors. In Proceedings of the 1995 IEEE 5th International Conference on Conduction and Breakdown in Solid Dielectrics, Leicester, England, 1995: 423–427.
[69] Singha S, Thomas MJ. Dielectric properties of epoxy nanocomposites. *IEEE T Dielect El In* 2008, **15**: 12–23.